15. Kuwahara, C., A. M. Takeuchi, T. Nishimura, K. Haraguchi, A. Kubosaki, Y. Matsumoto, K. Saeki, Y. Matsumoto, T. Yokoyama, S. Itohara, and T. Onodera. 1999. Prions prevent neuronal cell-line death. *Nature* 400: 225–226.
16. Imaoka, K., M. Kimura, M. Suzuki, T. Kamiyama, and A. Yamada. 2007. Simultaneous detection of the genus *Brucella* by combinatorial PCR. *Jpn. J. Infect. Dis.* 60: 137–139.
17. Watarai, M., S. Makino, Y. Fujii, K. Okamoto, and T. Shirahata. 2002. Modulation of *Brucella*-induced macropinocytosis by lipid rafts mediates intracellular replication. *Cell. Microbiol.* 4: 341–355.
18. Kim, C. L., A. Umetani, T. Matsui, N. Ishiguro, M. Shinagawa, and M. Horiuchi. 2004. Antigenic characterization of an abnormal isoform of prion protein using a new diverse panel of monoclonal antibodies. *Virology* 320: 40–51.
19. Prusiner, S. B. 1982. Novel proteinaceous infectious particles cause scrapie. *Science* 216: 136–144.
20. Isaacs, J. D., G. S. Jackson, and D. M. Altmann. 2006. The role of the cellular prion protein in the immune system. *Clin. Exp. Immunol.* 146: 1–8.
21. Fontes, P., M. T. Alvarez-Martinez, A. Gross, C. Carnaud, S. Köhler, and J. P. Liautard. 2005. Absence of evidence for the participation of the macrophage cellular prion protein in infection with *Brucella suis*. *Infect. Immun.* 73: 6229–6236.
22. Edenhofer, F., R. Rieger, M. Famulok, W. Wendler, S. Weiss, and E. L. Winnacker. 1996. Prion protein PrPc interacts with molecular chaperones of the Hsp60 family. *J. Virol.* 70: 4724–4728.
23. Linden, R., Y. Cordeiro, and L. M. Lima. 2012. Allosteric function and dysfunction of the prion protein. *Cell. Mol. Life Sci.* 69: 1105–1124.
24. Kaufmann, S. H. 1990. Heat shock proteins and the immune response. *Immunol. Today* 11: 129–136.
25. Hoffman, P. S., and R. A. Garduno. 1999. Surface-associated heat shock proteins of *Legionella pneumophila* and *Helicobacter pylori*: roles in pathogenesis and immunity. *Infect. Dis. Obstet. Gynecol.* 7: 58–63.
26. Frisk, A., C. A. Ison, and T. Lagergård. 1998. GroEL heat shock protein of *Haemophilus ducreyi*: association with cell surface and capacity to bind to eukaryotic cells. *Infect. Immun.* 66: 1252–1257.
27. Ensgraber, M., and M. Loos. 1992. A 66-kilodalton heat shock protein of *Salmonella typhimurium* is responsible for binding of the bacterium to intestinal mucus. *Infect. Immun.* 60: 3072–3078.
28. Hennequin, C., F. Porcheray, A. Waligora-Dupriet, A. Collignon, M. Barc, P. Bourlioux, and T. Karjalainen. 2001. GroEL (Hsp60) of *Clostridium difficile* is involved in cell adherence. *Microbiology* 147: 87–96.
29. Kiriya, K., N. Watanabe, A. Nishio, K. Okazaki, M. Kido, K. Saga, J. Tanaka, T. Akamatsu, S. Ohashi, M. Asada, et al. 2007. Essential role of Peyer's patches in the development of *Helicobacter*-induced gastritis. *Int. Immunol.* 19: 435–446.
30. Baorto, D. M., Z. Gao, R. Malaviya, M. L. Dustin, A. van der Merwe, D. M. Lublin, and S. N. Abraham. 1997. Survival of FimH-expressing enterobacteria in macrophages relies on glycolipid traffic. *Nature* 389: 636–639.

Downloaded from http://jimmunol.org/ at National Institute of Infectious Disease on February 12, 2013

OPEN ACCESS Freely available online

PLOS ONE

Early Detection of Abnormal Prion Protein in Genetic Human Prion Diseases Now Possible Using Real-Time QUIC Assay

Kazunori Sano[1,8], Katsuya Satoh[1]*, Ryuichiro Atarashi[1,9], Hiroshi Takashima[2], Yasushi Iwasaki[3], Mari Yoshida[3], Nobuo Sanjo[4], Hiroyuki Murai[5], Hidehiro Mizusawa[4], Matthias Schmitz[6], Inga Zerr[6], Yong-Sun Kim[7], Noriyuki Nishida[1,8]

1 Department of Molecular Microbiology and Immunology, Nagasaki University Graduate School of Biomedical Sciences, Nagasaki, Japan, **2** Department of Neurology and Geriatrics, Kagoshima University Graduate School of Medical and Dental Sciences, Kagoshima, Japan, **3** Department of Neuropathology, Institute for Medical Science of Aging, Aichi Medical University, Aichi, Japan, **4** Department of Neurology and Neurological Science, Graduate School, Tokyo Medical and Dental University, Tokyo, Japan, **5** Department of Neurology, Iizuka Hospital, Fukuoka, Japan, **6** Dementia Research Unit, National Reference Center for TSE, Georg-August University, Göttingen, Germany, **7** Ilsong Institute of Life Science, Hallym University, Gyeonggi-Do, Republic of Korea, **8** Global Centers of Excellence Program, Nagasaki University, Nagasaki, Japan, **9** Nagasaki University Research Centre for Genomic Instability and Carcinogenesis, Nagasaki University, Nagasaki, Japan

Abstract

Introduction: The definitive diagnosis of genetic prion diseases (gPrD) requires pathological confirmation. To date, diagnosis has relied upon the finding of the biomarkers 14-3-3 protein and total tau (t-tau) protein in the cerebrospinal fluid (CSF), but many researchers have reported that these markers are not sufficiently elevated in gPrD, especially in Gerstmann-Sträussler-Scheinker syndrome (GSS). We recently developed a new *in vitro* amplification technology, designated "real-time quaking-induced conversion (RT-QUIC)", to detect the abnormal form of prion protein in CSF from sporadic Creutzfeldt-Jakob disease (sCJD) patients. In the present study, we aimed to investigate the presence of biomarkers and evaluate RT-QUIC assay in patients with gPrD, as the utility of RT-QUIC as a diagnostic tool in gPrD has yet to be determined.

Method/Principal Findings: 56 CSF samples were obtained from gPrD patients, including 20 cases of GSS with P102L mutation, 12 cases of fatal familial insomnia (FFI; D178N), and 24 cases of genetic CJD (gCJD), comprising 22 cases with E200K mutation and 2 with V203I mutation. We subjected all CSF samples to RT-QUIC assay, analyzed 14-3-3 protein by Western blotting, and measured t-tau protein using an ELISA kit. The detection sensitivities of RT-QUIC were as follows: GSS (78%), FFI (100%), gCJD E200K (87%), and gCJD V203I (100%). On the other hand the detection sensitivities of biomarkers were considerably lower: GSS (11%), FFI (0%), gCJD E200K (73%), and gCJD V203I (67%). Thus, RT-QUIC had a much higher detection sensitivity compared with testing for biomarkers, especially in patients with GSS and FFI.

Conclusion/Significance: RT-QUIC assay is more sensitive than testing for biomarkers in gPrD patients. RT-QUIC method would thus be useful as a diagnostic tool when the patient or the patient's family does not agree to genetic testing, or to confirm the diagnosis in the presence of a positive result for genetic testing.

Citation: Sano K, Satoh K, Atarashi R, Takashima H, Iwasaki Y, et al. (2013) Early Detection of Abnormal Prion Protein in Genetic Human Prion Diseases Now Possible Using Real-Time QUIC Assay. PLoS ONE 8(1): e54915. doi:10.1371/journal.pone.0054915

Editor: Andrew Francis Hill, University of Melbourne, Australia

Received August 9, 2012; **Accepted** December 17, 2012; **Published** January 25, 2013

Copyright: © 2013 Sano et al. This is an open-access article distributed under the terms of the Creative Commons Attribution License, which permits unrestricted use, distribution, and reproduction in any medium, provided the original author and source are credited.

Funding: This study was supported by Grants-in-Aid from the Research Committee of Surveillance and Infection Control of Prion Disease and from the Research Committee of Prion Disease and Slow Virus Infection, the Ministry of Health, Labour and Welfare of Japan. Dr. Sano and Professor Nishida are supported by the Global COE Program for tropical and emerging diseases, Nagasaki University, Japan. Dr. Satoh has received research support from Grant-in Aid for Scientific Research (C) (24591268) and from the Ministry of Education, Culture, Sports, Science and Technology and Japan Society for the Promotion of Science. This work was supported by Grants-in-Aid from the Research Committee on Surveillance and Infection Control of Prion Disease, the Ministry of Health, Labour and Welfare of Japan. Dr. Atarashi has received research support from Grant-in-Aid for Scientific Research (B) (23300127) from the Ministry of Education, Culture, Sports, Science and Technology of Japan, and a grant from the Ministry of Health, Labour, and Welfare, and a grant from Takeda Science Foundation. Dr. Sano has received research support from Grant-in-Aid for Young Scientific Research (B) (23790998) from the Ministry of Education, Culture, Sports, Science and Technology of Japan. The funders had no role in study design, data collection and analysis, decision to publish, or preparation of the manuscript.

Competing Interests: The authors have declared that no competing interests exist.

* E-mail: satoh-prion@nagasaki-u.ac.jp

Introduction

Prion diseases (PrD) are fatal neurodegenerative disorders characterized by the accumulation of abnormal prion protein (PrP^{Sc}) in the CNS. The genetic form of human PrD (gPrD) is caused by mutations in the *prion protein gene* (*PRNP*), and is classified into genetic CJD (gCJD), Gerstmann-Sträussler-Scheinker syndrome (GSS), and fatal familial insomnia (FFI). Patients with GSS and FFI have symptoms such as dementia, dyskinesia and sleep disorders, but show no specific signal in diffusion-weighed MR imaging, and therefore the clinical discrimination of GSS and FFI from non-prion diseases such as spinocerebellar degeneration (SCA) [1] and chronic refractory sleep disorders, respectively, is problematic.

Table 1. Summary of CSF analysis of genetic prion disease cases.

	GSS	FFI	g CJD	
	P102L	D178N	E200K	V203I
Number	20	12	22	2
Age (average year)	55.5±4.45	55.8±13.7	62.7±9.43	73
Sex (m:f)	1:3	3:1	1:1	2:0
positive patients/total (%)				
[95% CI*]				
	4/20	1/12	19/22	1/2
t-tau protein	(20%)	(8.3%)	(86.3%)	(50%)
	[2.6–37.4%]	[0–25.4%]	[70.2–100%]	
	4/20	1/12	18/22	1/2
14-3-3 protein	(20%)	(8.3%)	(81.8%)	(50%)
	[2.6–37.4%]	[0–25.4%]	[67.4–96.2%]	
	18/20	10/12	18/22	2/2
RT-QUIC	(90%)	(83.3%)	(81.8%)	(100%)
	[76.5–100%]	[70.2–100%]	[67.4–96.2%]	

*The 95% confidence interval [CI] was calculated using the adjusted Wald test, and was expressed only in groups of more than seven cases.

doi:10.1371/journal.pone.0054915.t001

We recently developed a new *in vitro* amplification technology, designated "real-time quaking-induced conversion (RT-QUIC)", for the detection of PrP^{Sc} in CSF of sCJD [2]. The aim of the present study was to determine whether RT-QUIC could also be of value in patients with genetic prion disease, as well as in sCJD.

Materials and Methods

Patients

We retrospectively analyzed 56 CSF samples obtained from gPrD patients in Japan, South Korea and Germany, including 22 cases of E200K gCJD, 20 cases of P102L GSS, 12 cases of FFI and 2 cases of V203I gCJD (Table1). PrP-genotyping was done using genomic DNA extracted from peripheral blood leukocytes, as described previously [3]. Informed consent was obtained from patients' families and/or patients. The study protocol was approved by the Ethics Committee of Nagasaki University Hospital (ID: 10042823) and registered with the University Hospital Medical Information Network (ID: UMIN000003301).

Real-time QUIC and analysis of 14-3-3 and t-t-tau protein in CSF samples

We analyzed all CSF samples by RT-QUIC method as previously described [2]. 14-3-3 proteins in CSF were analyzed by Western blotting and total-tau protein was measured using an ELISA kit (INNOTEST®) as previously described [3].

Expression and purification of recombinant human PrP

Recombinant PrP, equivalent to residues 23–231 of the human PrP sequence, (codon 129 M) was expressed, refolded into a soluble form (rHuPrP-sen), and purified essentially as described previously [2]. The concentration of rHuPrP-sen was determined by measuring the absorbance at 280 nm. The purity of the final protein preparations was ≥99%, as estimated by SDS-PAGE, immunoblotting, and liquid chromatography-mass spectrometry. Circular dichroism analysis showed the conformation of rHuPrP-sen was α-helix-rich (data not shown). After purification, aliquots of the proteins were stored at −80°C in 10 mM phosphate buffer, pH 6.8.

Real-time QUIC

We prepared reactions in a black 96-well optical bottom plate (Nunc, Rochester, NY, USA) to a final volume of 100 µl. To avoid contamination, we prepared non-infectious materials inside a biological safety cabinet in a prion-free laboratory and used aerosol-resistant tips. The final concentrations of reaction buffer components were 500 mM NaCl, 50 mM PIPES pH 7.0, 1 mM EDTA and 10 µM Thioflavin T. The rHuPrP-sen concentration was 50 µg/ml, and only freshly-thawed rHuPrP-sen was used. CSF (5 µl per well) was used to seed the RT-QUIC reactions. The 96-well plate was covered with sealing tape (Nunc 236366) and incubated at 37°C in a plate reader (Infinite M200 or F200 fluorescence plate reader; TECAN) with intermittent shaking, consisting of 30 s circular shaking at the highest speed and no shaking for 30 s, with a 2 min pause to measure the fluorescence. The kinetics of fibril formation was monitored by reading the fluorescence intensity every 10 min using 440 nm excitation and 485 nm emission and monochromators (Infinite M200) or filters (Infinite F200).

Results (Figure 1, Table 1, 2 and 3)

First we analyzed 22 CSF samples from E200K gCJD patients. The positivities of t-tau protein, 14-3-3 protein and RT-QUIC method were all in the range of 80–85% (Figure 1, Table 1, 2 and 3). Overall, PrP^{Sc} was detected in 18 of the cases by RT-QUIC, all of which were also positive for both t-tau and 14-3-3 proteins. In the GSS and FFI cases, RT-QUIC was positive in 90% of GSS and 83.3% of FFI (Figure 1 and Table1 and 2). Among the GSS cases, however, 80% showed negative for both t-tau and 14-3-3 proteins, and all but one of the FFI samples were negative for the biomarkers (Figure 1, Tables 1 and 2). Although we were able to analyze only 2 cases of gCJD V203I, both were positive by RT-QUIC and only one was positive for the biomarkers. All gPrD patients were methionine homozygotes at codon 129 of *PRNP*.

We compared the kinetics of recombinant Human PrP (rHuPrP) fibril formation in CSF of sCJD patients with those of gPrD patients, and found no significant difference (Figure 1).

Discussion

The RT-QUIC in vitro PrP^{Sc} amplification assay for diagnosis of prion disease has shown 84% sensitivity and 100% specificity in CSF samples from sporadic CJD patients.

To determine the value of RT-QUIC in genetic prion disease diagnosis, we analyzed a total of 56 CSF samples from patients with various genetic forms of human prion disease (Table 1). Our study demonstrated that RT-QUIC was highly positive in all four of the gPrD types we analyzed. Notably, most of the GSS and FFI patients were negative for both 14-3-3 and t-tau, as found in previous studies [4], whereas RT-QUIC showed 90% positivity in GSS.

RT-QUIC method was capable of detecting an extremely low volume of PrP^{Sc}, and we were able to detect as little as ≥1 fg of PrP^{Sc} in diluted brain homogenate from sCJD patients. While we were not able to detect PrP^{Sc} in all sCJD CSF samples, the reasons for this are unclear and we assume that the amounts of PrP^{Sc} are very much lower in CSF samples of negative gPrD patients.

Because the majority of GSS patients remain alive with only relatively mild symptoms one year after the onset [5], many

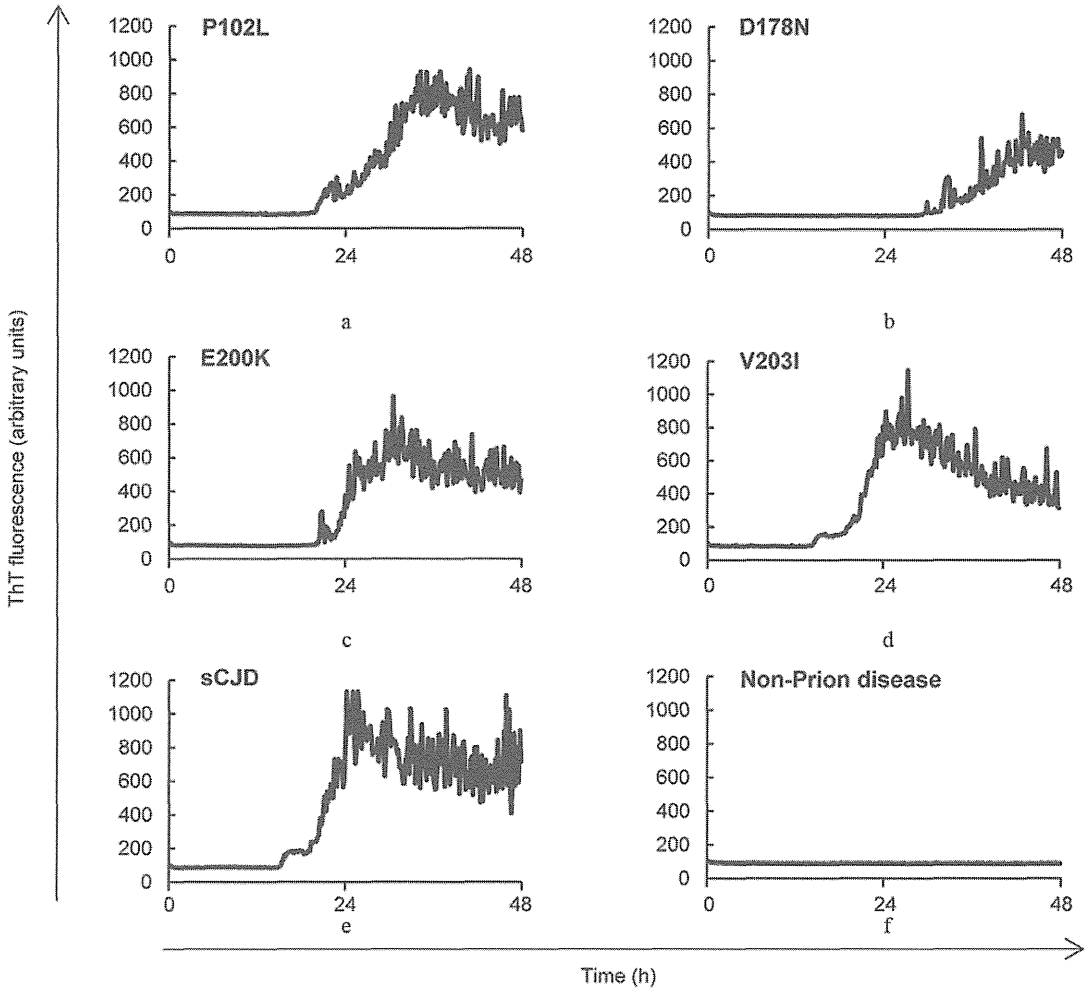

Figure 1. The kinetics of rHuPrP fibril formation with seeds from CSF of GSS, FFI, or gCJD. (**a**) a GSS P102L patient (**b**) a FFI D178N patient (**c**) a gCJD E200K patient (**d**) a gCJD V203I patient (**e**) a sCJD (MM1) patient and (**f**) a control subject.
doi:10.1371/journal.pone.0054915.g001

Table 2. Further analysis of CSF samples of P102L GSS patients.

	duration between the symptom onset and lumbar puncture	
	1–12 months	13–77 months
Number	8 samples	12 samples
Age (average year)	56.8±2.14	54.9±5.19
Sex (m:f)	3:5	2:10
positive patients/total (%)		
t-tau protein	3/8	1/12
	37.5%	8.3%
14-3-3 protein	3/8	1/12
	37.5%	8.3%
RT-QUIC	8/8	10/12
	100%	83.3%

doi:10.1371/journal.pone.0054915.t002

Table 3. Further analysis of CSF samples of gCJD E200K patients.

	duration between the symptom onset and lumbar puncture	
	1–3 months	4–48 months
Number	10 samples	12 samples
Age (average year)	61.4±8.96	63.8±9.67
Sex (m:f)	7:3	1:2
positive patients/total patients(%)		
t-tau protein	9/10	10/12
	90.0%	83.3%
14-3-3 protein	8/10	10/12
	80.0%	83.3%
RT-QUIC	7/10	11/12
	70.0%	91.6%

doi:10.1371/journal.pone.0054915.t003

consult a clinician only later in the disease progression. On other hand, the progression of CJD is much more rapid, with most patients exhibiting akinetic mutism within 3 months. For this reason, we define the "early stage" in GSS (P102L) as 1–12 months, and in E200K gCJD as 0–3 months.

Moreover GSS and FFI show considerable phenotypic variability [6,7], and it is very important to distinguish them from non-prion diseases at an early stage. Until now, this has not been possible. Using the RT-QUIC assay, however, we were able to confirm positivity in 100% of GSS patients at an early stage, prior to disease progression (Table 2). Thus, RT-QUIC has application in the laboratory detection of gPrD as well as sCJD, and is likely to be of particular advantage in the differential diagnosis of FFI and GSS, in which biomarkers are usually negative (Tables 2 and 3).

Interestingly, one patient with E200K gCJD was negative by RT-QUIC when sampled at 2 months after the symptom onset, but became positive when a second sample was obtain two months later. Thus, it is important that even if the CSF analysis by RT-QUIC is negative at an early stage, it should be re-examined at a later time point. Additionally, the use of RT-QUIC along with testing for the biomarkers should prove valuable for monitoring clinical trials of therapeutic agents use in gPrD patients.

We believe that RT-QUIC analysis of CSF will become invaluable in the differential diagnosis of suspected prion diseases, since not all patients with the genetic mutation go on to develop prion diseases. Alpha

In conclusion, RT-QUIC enables the early diagnosis of GSS and FFI in many patients for whom a differential diagnosis is otherwise not currently possible.

Author Contributions

Conceived and designed the experiments: K. Satoh K. Sano RA NN. Performed the experiments: K. Sano K. Satoh RN. Analyzed the data: K. Satoh. Contributed reagents/materials/analysis tools: HT YI MY NS H. Murai H. Mizusawa MS IZ YK. Wrote the paper: K. Sano K. Satoh RN NN.

References

1. Popova SN, Tarvainen I, Capellari S, Parchi P, Hannikainen P, et al. (2012) Divergent clinical and neuropathological phenotype in a Gerstmann-Straussler-Scheinker P102L family. Acta Neurol Scand; 126(5): 315–23
2. Atarashi R, Satoh K, Sano K, Fuse T, Yamaguchi N, et al. (2011) Ultrasensitive human prion detection in cerebrospinal fluid by real-time quaking-induced conversion. Nat Med; 17: 175–178.
3. Satoh K, Tobiume M, Matsui Y, Mutsukura K, Nishida N, et al. (2010) Establishment of a standard 14-3-3 protein assay of cerebrospinal fluid as a diagnostic tool for Creutzfeldt-Jakob disease. Lab Invest; 90: 1637–1644.
4. Ladogana A, Sanchez-Juan P, Mitrová E, Green A, Cuadrado-Corrales N, et al. (2009) Cerebrospinal fluid biomarkers in human genetic transmissible spongiform encephalopathies. J Neurol; 256: 1620–1628.
5. Webb TE, Poulter M, Beck J, Uphill J, Adamson G, et al. (2008) Phenotypic heterogeneity and genetic modification of P102L inherited prion disease in an international series. Brain; 131 (Pt 10): 2632–2646.
6. Capellari S, Strammiello R, Saverioni D, Kretzschmar H, Parchi P. (2011) Genetic Creutzfeldt-Jakob disease and fatal familial insomnia: insights into phenotypic variability and disease pathogenesis. Acta Neuropathol; 121(1): 21–37.
7. Piccardo P, Dlouhy SR, Lievens PM, Young K, Bird TD, et al. (1998) Phenotypic variability of Gerstmann-Straussler-Scheinker disease is associated with prion protein heterogeneity. J Neuropathol Exp Neuro; 57(10): 979–988.

JVI Accepts published online ahead of print

JVI Accepts, published online ahead of print on 29 February 2012
J. Virol. doi:10.1128/JVI.06326-11
Copyright © 2012, American Society for Microbiology. All Rights Reserved.

Protective role of interferon regulatory factor3-mediated signaling against prion infection

Running title: Role of IRF3 in prion infection

Daisuke Ishibashi[1]*, Ryuichiro Atarashi[1,3], Takayuki Fuse[1], Takehiro Nakagaki[1], Naohiro Yamaguchi[1], Katsuya Satoh[1], Kenya Honda[2] and Noriyuki Nishida[1,4]

1. Department of Molecular Microbiology and Immunology, Nagasaki University Graduate School of Biomedical Sciences, 1-12-4 Sakamoto, Nagasaki 852-8523, Japan.
2. Department of Immunology, Graduate School of Medicine and Faculty of Medicine, University of Tokyo, Hongo 7-3-1, Bunkyo-ku, Tokyo 113-0033, Japan.
3. Nagasaki University Research Centre for Genomic Instability and Carcinogenesis, Nagasaki, Japan.
4. Global Centers of Excellence Program, Nagasaki University, Nagasaki, Japan.
*: Corresponding author: Daisuke Ishibashi,
Department of Molecular Microbiology and Immunology, Nagasaki University Graduate School of Biomedical Sciences, 1-12-4 Sakamoto, Nagasaki 852-8523, Japan.
Tel.: +81-95-819-7059
Fax: +81-95-819-7060
E-mail: dishi@nagasaki-u.ac.jp

Keywords: prion, innate immunity, interferon regulatory factor 3 (IRF3)

JVI Accepts published online ahead of print

ABSTRACT

Abnormal prion protein (PrP^{Sc}) generated from the cellular isoform of PrP (PrP^{C}) is assumed to be the main or sole component of the pathogen, called prion, of transmissible spongiform encephalopathies (TSE). Because PrP is a host-encoded protein, acquired immune responses are not induced in TSE. Meanwhile, activation of the innate immune system has been suggested to partially block the progression of TSE; however, the mechanism is not well understood. To further elucidate the role of the innate immune system in prion infection, we investigated the function of interferon regulatory factor 3 (IRF3), a key transcription factor of the MyD88-independent type I interferon (IFN) production pathway. We found that IRF3-deficient mice exhibited significantly earlier onset with three murine TSE strains, namely, 22L, FK-1, and mBSE following intraperitoneal transmission, when compared with wild-type controls. Moreover, overexpression of IRF3 attenuated prion infection in the cell culture system, while PrP^{Sc} was increased in prion-infected cells treated with small interfering RNAs (siRNA) against IRF3, suggesting that IRF3 negatively regulates PrP^{Sc} formation. Our findings provide new insight into the role of the host innate immune system in the pathogenesis of prion diseases.

JVI Accepts published online ahead of print

INTRODUCTION

Transmissible spongiform encephalopathies (TSE) are fatal zoonoses, and include Creutzfeldt–Jakob disease (CJD) in humans, and scrapie and bovine spongiform encephalopathy (BSE) in animals. All exhibit the three major histopathological features of spongiform change, neuronal loss and gliosis in the central nervous system (CNS) (30). The infectious agent, prion, is considered not to possess its own genome and to be composed mainly of the proteinase K (PK)-resistant and β-sheet-rich abnormal isoform of prion protein, designated PrP^{Sc}, which is generated by conformational conversion of the normal form of PrP (PrP^{C}) (43). In contrast to conventional pathogens, such as bacteria and virus, acquired immunity against prion infection is not elicited, probably because PrP is a host-encoded protein, resulting in immunotolerance to PrP^{Sc} (1).

Prior to activation of acquired immune responses, the invasion of pathogens, including bacteria and viruses, is first recognized by the innate immune system, with the switching on of the cellular defense system leading to the production of cytokines and interferons (IFNs). The innate immune responses are initiated through both toll-like receptors (TLRs) (2) and intracellular sensor molecules such as retinoic acid inducible gene-I (RIG-I) and melanoma differentiation associated gene-5 (MDA5), each of which recognizes specific components of foreign pathogens, namely pathogen-associated molecular patterns (PAMPs) (20). In addition, the innate immunity is the main system contributing to inflammation caused by microbial infection or tissue damage (3, 8). Since gliosis, a major characteristic of TSE, is thought to be a kind of inflammatory response, it is reasonable to assume that innate immunity may play a role in the pathogenesis of TSE. Indeed, it was reported that pretreatment with complete Freund's adjuvant (CFA) (39) or unmethylated CpG DNA (35), both of which activate innate immunity through TLRs, delays the onset of TSE in mice inoculated with mouse-adapted scrapie prion, suggesting that activation of innate immunity is protective against prion infection. In contrast, deletion of MyD88 gene, which is an essential intracellular signal transducer in all TLRs except for TLR3, has been shown not to significantly affect incubation time in the same mouse scrapie model (29). Thus, MyD88-dependent signaling pathways are unlikely to be implicated in prion infection in the absence of forced activation of innate immune responses by conventional PAMPs (2, 20). On the other hand, mice that possess a non-functioning mutation of TLR4, which activates not only MyD88-dependent but also MyD88-independent (also called

JVI Accepts published online ahead of print

TRIF-dependent) pathway, develop scrapie earlier than control mice (36). Accordingly, it is suggested that blockade of TLR4 signaling pathway accelerates the progression of TSE. Nonetheless, the effects of the innate immune system on prion infection remain controversial and have not been fully clarified.

We focus on interferon regulatory factor 3 (IRF3), which is a key transcription factor of the MyD88-independent pathway that has an essential role in the type I IFN response to microbial infection, and whose deficiency in mice leads to susceptibility to many viruses (19). In this study, we investigated the role of IRF3 in prion infection using IRF3-deficient mice and prion-susceptible cell lines.

RESULTS

Prion infection is accelerated in IRF3-deficient mice.

To clarify the significance of IRF3-dependent signaling pathways in prion infection *in vivo*, we peripherally inoculated 22L strain into IRF3-gene knockout mice (IRF3-/-) (33) and control wild-type (C57BL/6) mice. When the mice were challenged with 10^{-3} dilution of 22L inoculum by the intraperitoneal (i.p.) route, the IRF3-/- mice showed significantly abbreviated survival periods (257 ± 8 days, $p < 0.001$) compared with those of the control mice (281 ± 15 days) (Table 1 and Fig. 1A). To further investigate the protective effect of IRF3 on prion infection, the mice were challenged with 10^{-3} dilution of mouse-adapted BSE (mBSE) or Fukuoka 1 (FK-1) strain by the i.p. route. IRF3-/- mice showed shorter survival periods of mBSE (335 ± 37 versus 380 ± 33 days, $p < 0.05$), and FK-1 (251 ± 31 versus 321 ± 24 days, $p < 0.01$) compared with control mice (Table 1). The shortening of survival periods in the IRF3-/- mice is unlikely to be due to developmental defects in the brains or lymphoreticular organs, because IRF3-/- mice were shown to have normal lymphocyte populations in the thymus and spleen (33). Moreover, immunostaining with anti-follicular dendritic cell (FDC) antibody (CNA.42) (31) was performed to compare the FDC population in the spleen between IRF3-/- and wild-type mice. Staining reactions were similar in the two groups (Fig. 4B).

We examined for the presence of PrP^{Sc} in the brain tissues of terminal-stage infected with 22L prion strain by Western blotting. The levels of PrP^{Sc} in IRF3-/- mice at 32 weeks post-infection (w.p.i.) were equivalent to those of wild-type mice at 40 w.p.i. (Fig. 1B). Moreover, no significant differences were observed between wild-type mice and IRF3-/- mice in the accumulation of PrP^{Sc} in the lesion profiles of

JVI Accepts published online ahead of print

PrP-immunostaining (Fig. 1C). Because spongiform changes and gliosis are common characteristics of prion diseases, brain sections including the cerebral cortex (Cx), hippocampus (Hi), thalamus (TH), cerebellum (CE), and pons (Po) from 22L-inoculated mice were examined by histologically and subjected to immunohistochemical analysis using anti-Iba-1 antibodies for microgliosis (Fig. 3A) or ant-GFAP for astrogliosis (Fig. 3B). The severity and distribution of vacuolation and glial activation in the IRF3-/- mice at 32 w.p.i. were indistinguishable from those in the wild-type mice at 40 w.p.i. (Fig 2 and 3), while IRF3-/- mice displayed significantly increased vacuolation (Fig. 2) and astrogliosis (Fig. 3B) in the Cx and CE at 25 w.p.i.. Collectively, these results suggest that the progression of TSE following i.p. transmission is accelerated in IRF3-/- mice, although genetic elimination of IRF3 does not affect the final neuropathological outcome. Furthermore, as shown in Table 2 and Fig. 4A, the deposition of PrP^{Sc} in the white pulp region of the spleens from the IRF3-/- mice was detectable in 1/5 at 2 w.p.i., 4/5 at 5 w.p.i., and 5/5 at 8 w.p.i., whereas none of the wild-type mice was positive at the same timepoints. These observations indicate that the rate of accumulation of PrP^{Sc} in the spleen was enhanced in the IRF3-/- mice.

IRF3-dependent pathway is protective against prion infection in cell culture.

We tested whether overexpression of IRF3 could affect the production of PrP^{Sc} in the cell culture models. The level of PrP^{C} was not affected by the transient expression of the genes in uninfected N2a58 cells (data not shown). PrP^{Sc} was significantly decreased by overexpression of IRF3 in the 22L-N2a58 cells (Fig. 5A). We confirmed that the activated form of IRF3 (phosphorylated at Ser396 of IRF3) increases in a dose-dependent manner after transfection of the IRF3 gene in both 22L-N2a58 cells (Fig. 5A) and uninfected N2a58 cells (data not shown), indicating that the up-regulation of IRF3-phosphrylation seen in the Fig. 5A is most likely due to an increase in the level of IRF3 protein after transfection.

To investigate the effect of down-regulation of IRF3 in the 22L-N2a58 cells, we performed knockdown experiments using small interfering RNAs (siRNA). IRF3 expression was significantly decreased by two types of siRNA against IRF3, whereas β-actin expression, as the internal standard, was not changed (Fig. 5B). Application of siRNA did not influence the expression of PrP^{C} in N2a58 cells (data not shown), whereas the level of PrP^{Sc} was increased in 22L-N2a58 cells treated with siRNA against

JVI Accepts published online ahead of print

IRF3 (Fig. 5B). These data suggest that IRF3 has an inhibitory effect on the production of PrP^{Sc} in the 22L-N2a58 cells.

To further evaluate the protective effect of IRF3, we established cell clones stably expressing HA-tagged IRF3 using another mouse PrP-overexpressed N2a cell clone (designated N2a75). Several HA-IRF3-negative and -positive clones were isolated by selection for resistance to hygromycin. HA-tagged IRF3 was expressed in clones A4, C1, and H3, which were accompanied by an increase in total IRF3 protein, while clones A1 and E1 were negative (Fig. 5C). After incubation with 22L-infected BH, the cell clones were subcultured for 5 passages, and analyzed by Western blotting with anti-PrP antibodies. The levels of PrP^{Sc}/PrP^{C} ratio were inversely correlated with the levels of IRF3/beta-actin ratio (Fig. 5C), indicating that enhanced expression of IRF3 effectively blocks new prion infection.

DISCUSSION

In the present study, we found that a genetic deficiency of IRF3 accelerates the progression of TSE following i.p. transmission in mice and the accumulation rate of PrP^{Sc} in the spleen is increased in the IRF3-/- mice. Furthermore, we demonstrated that IRF3 has the inhibitory effect on the PrP^{Sc} accumulation and the levels of IRF3 are inversely correlated with resistance to prion infection in cell culture.

IRF-3 is known to be constitutively expressed in many tissues and cells (6, 22, 45). Indeed, we confirmed the expression of IRF3 in brains (data not shown) and the N2a58 cells (Fig. 5). Furthermore, not only glial cells but also neurons express most innate immunity-related genes and produce type I IFN in response to virus infection (11). Although the role of IRF3 in prion propagation into the CNS is still unclear, we speculate that an absence of IRF-3 signaling leads to increased prion replication not only in peripheral tissues but also in the CNS. It would be of great value to examine this further using neuron-specific IRF3-disrupted mice or neuron-specific IRF3-expressing mice.

It was reported, in prion infection, that genetic disturbance of TLR4 (36) or IL-10 (41) leads to shorter incubation periods of prion infection. Since these, respectively, are an upstream and a downstream factor of IRF3-mediated pathway, the findings may be due in part to functional changes in the IRF3-mediated signaling.

Based on these results, two hypothetical models are proposed to explain the inhibitory

JVI Accepts published online ahead of print

effect of IRF3 on the prion infection. The first is that MyD88-independent "pattern recognition receptors (PRRs)" such as TLR3, TLR4 or RIG-I/MDA5 might recognize prion, and the resulting activation of IRF3 could induce various IRF3-responsive genes that may participate in the protective effect. The fact that the *in vivo* administration of IFNs, a representative of the IRF3-responsive genes, previously failed to show inhibitory effects on TSE (13, 16) suggests that IRF3-responsive genes other than IFNs may be important for the inhibitory effect of IRF3 on prion infection. Of note, the protective effect of IRF3 against several viruses has been suggested to be largely independent of the production of type I-IFN, and probably responsible for the anti-viral actions of specific IRF3-responsive genes (10, 18, 21). Peritoneal macrophages from wild-type mice moderately induced TNF-α or IL-6 following exposure to PrP^{Sc}-mimicking PrP peptides (PrP106–126 or PrP118–135), whereas TLR4 signaling-mutant mice were impaired in their ability to produce these cytokines (36), supporting in part the hypothesis that some PRRs may sense PrP^{Sc} as a sort of PAMP. On the other hand, it should be noted that the MyD88-independent pathway activates both NF-κB and IRF3. Although the induction of proinflammatory cytokines essentially depends upon NF-κB, it was unclear whether the activation of IRF3 was induced by these PrP peptides. In fact, the hallmarks of IRF3 activation, such as phosphorylation, dimerization and cytoplasm-to-nucleus translocation of IRF3 in 22L-N2a58 cells were not detected (data not shown). Moreover, it was previously reported that IFNs were not detected in the serum, spleens, or brains of mice infected with scrapie (44). In addition, IFN-β mRNA does not increase in the brains of CJD patients (7) or mice infected with ME7 prion strain (14). Hence, these results argue against the notion that the IRF3-mediated signaling is activated by prion infection, but it remains to be determined whether transient and weak responses are evoked at an early phase in the infection. The question as to whether IRF3-mediated signaling directly suppresses the production of PrP^{Sc} or increases its degradation also remains open.

Another explanation is that prion infection itself may have little effect on the pathway, but that the basal activity of IRF3 may have some degree of inhibitory effect on prion propagation. It has been reported that IRF3 can be activated not only by viruses but also by multiple activators such as cellular stress and DNA damage (24) (34). Accordingly, it is possible that constitutive activation of IRF3, albeit at a low level, occurs in the brain even in the absence of a pathogen. This notion is further supported

JVI Accepts published online ahead of print

by the fact that constitutive, weak IFN-signaling in the absence of viral infection plays a role in modifying cellular responsiveness in the immune and other biological systems (38, 40). Accumulating evidence indicates that many viruses have evolved to evade the innate immune system, including IRF3-mediated signaling (15, 23). For instance, an active mutant of IRF3 has been reported to exert a markedly suppressive effect on cellular HIV-1 infection and administration of poly I:C potently inhibits HIV-1 replication in microglia through a pathway requiring IRF3. Nonetheless, HIV-1 itself does not activate IRF3 but rather decreases IRF3 protein in HIV-1 infected cells (12, 37). Likewise, prion infection might disturb the activation of IRF3, even though prion is considered to be largely composed of PrP^{Sc}. We are currently investigating this possibility. Furthermore, an analogy can be made between the role of IRF3 in prion infection and that of IL-10. The levels of IL-10 are not increased in the brains of scrapie-infected mice (14, 42), whereas IL-10 knockout mice are highly susceptible to the development of scrapie (41).

In conclusion, we have shown that IRF3, a key transcription factor of the MyD88-independent pathways, operates in the host defense machinery against prion infection. The findings provide new insight into understanding of the innate immunity to prion infection.

MATERIALS AND METHODS

Reagents and Antibodies

The anti-PrP polyclonal mouse antiserum (SS) has been described previously (5). M20 is an affinity purified goat polyclonal antibody recognizing the C-terminus of mouse PrP (Santa Cruz Biotechnology, Inc., CA, USA). Anti-mouse IRF3 (Santa Cruz Biotechnology) and anti-mouse phospho-IRF3 (Ser396) (Cell Signaling Technology, Japan) were rabbit polyclonal antibodies, and anti-mouse β-actin (Sigma Aldrich, St. Louis, MO, USA) was a mouse monoclonal antibody. Horseradish peroxidase (HRP)-conjugated anti-goat immunoglobulin G antibody (Santa Cruz Biotechnology), anti-mouse and anti-rabbit IgG antibodies (Amersham Pharmacia Biotech AB, Uppsala, Sweden) were used for Western blotting.

Cell cultures

JVI Accepts published online ahead of print

The mouse neuroblastoma cell line N2a was purchased from the American Type Culture Collection (ATCC CCL131), and N2a58 cells overexpressing mouse PrP prepared from N2a were transfected with a plasmid carrying wild-type mouse prnp cDNA (PrP-a genotype, codons 108L and 189T) (27). Prion infected cells, 22L-N2a58, were produced as previously described (27). After limiting dilution, several PrP^{Sc}-positive clones were isolated. The cell clones producing the highest level of PrP^{Sc} were used for subsequent studies. The 22L-N2a58 cells stably expressed PrP^{Sc} for over 50 passages. The cells were cultured in DMEM (Sigma) containing 10% heat-inactivated fetal bovine serum and penicillin-streptomycin (Invitrogen, Carlsbad, CA, USA), and split every 3 days at a 1:10 ratio. All cultured cells were maintained at 37 °C in 5% CO_2 in the biohazard prevention area of the authors' institution.

Plasmid and siRNA

The mammalian expression pUNO vector contains a strong and ubiquitous composite promoter designated EF1α/HTLV. In this experiment, we inserted mouse IRF3 cDNA into multiple cloning sites of the pUNO vector (Invivogen, San Diego, CA, USA.). The HA-tagged mouse IRF3 cDNA was inserted into pcDNA3.1 vector (Invitrogen). The plasmids were introduced by Lipofectoamine LTX (Invitrogen) in the prion-infected cells and incubated for 48 h. The small interfering RNAs (siRNAs) were purchased from QIAGEN, Hilden, Germany. Two specific siRNA-targeted sequences (product IDs: SI00210770 and SI00210784) were used for IRF3 (according to GenBank accession No: NM016849), 5'- ACA GGT GGT GAT GGT TGG CAA -3' and 5'- GAC CCT TAT GAC CCT CAT AAA -3'. For the negative control, a siRNA (product ID: 1022076) targeting 5'- AAT TCT CCG AAC GTG TCA CGT-3' was used. The siRNAs were introduced into cells using Fugene 6 (Roche Diagnostics, Mannheim, Germany) and incubated for 48 h.

Western blotting

Samples were lysed with Triton-DOC lysis buffer (50 mM Tris-HCl [pH 7.5] containing 150 mM NaCl, 0.5% Triton X-100, 0.5% sodium deoxycholate, 2 mM EDTA, and protease inhibitors (Nakarai Tesque, Inc., Japan), for 30 min at 4 °C. After 1 min of centrifugation at 5000×g, the supernatant was collected and its total protein concentration was measured using the BCA protein assay kit (Pierce, Rockford, IL). To

JVI Accepts published online ahead of print

detect PrP^{Sc}, the protein concentration was adjusted to 10 mg/ml, and samples were digested with 20 μg/ml of proteinase K (PK, Sigma) at 37 °C for 30 min, and boiled for 5 min with sodium dodecyl sulfate (SDS) loading buffer (50 mM Tris-HCl, pH 6.8, containing 5% glycerol, 1.6% SDS, and 100 mM dithiothreitol) and subjected to SDS–polyacrylamide gel electrophoresis. The proteins were transferred onto an Immobilon-P membrane (Millipore, MA, USA) in transfer buffer containing 15% methanol at 300 mA for 1 h, and the membrane was blocked with 5 % nonfat dry milk in TBST (10 mM Tris-HCl [pH 7.8], 100 mM NaCl, 0.1% Tween 20) for 1 h at room temperature and reacted with diluted primary antibodies. Immunoreactive bands were visualized by HRP-conjugated secondary antibodies, using an enhanced chemiluminescence system (Amersham). The detailed methods have previously been described (4). To quantify the signals, we measured the intensity of each band using the NIH image J software.

Establishment of stably IRF3-overexpressing cells and in vitro 22L scrapie infection experiments

To establish cell lines stably expressing IRF3, pcDNA3.1 plasmid containing HA-tagged IRF3 gene was transfected using Fugen 6 (Roche) into PrP^{C}-overexpressing N2a cells (N2a 75 cells) and cultured for 48 h. After the cells were treated with 350 μg/mL hygromycin (HygroGold, Invivogen) in culture medium for 4 days, the drug-resistant colonies were isolated. We used the HygroGold-selected N2a 75 cells transfected with empty vector as a negative control. Then, the cells were infected with 22L scrapie strain (final concentration, 0.02 or 0.2% brain homogenate) in a 6-well culture plate for 48 h, and subsequently passaged into a 75 cm^2-flask. Once confluent, the sub-cultures were diluted 10-fold (27). After treatment with 40 μg/mL PK, immunoblotting was done to detect PrP^{Sc}.

In vivo scrapie infection experiments

Four-week-old wild-type (+/+) and IRF3 knockout (-/-) male mice of the same C57BL/6-derived genetic background were intraperitoneally (i.p.) inoculated with 100 μL of 10^{-3} dilution of brain homogenate (BH) from mice terminally infected with 22L, Fukuoka-1 (FK-1) or mouse-adapted BSE (mBSE) strain (28). The IRF3-/- mice were obtained from Dr. T. Taniguchi's group (Tokyo University) (33). As a negative

JVI Accepts published online ahead of print

(mock-infected) control, age- and strain-matched mice were inoculated i.p. with normal mouse BH. The spleens and brains of the mice were removed at 1, 2, 5, 8, 25 weeks post-infection (w.p.i.) and at the terminal stage of disease. Animals were cared for in accordance with the Guidelines for Animal Experimentation of Nagasaki University.

Histopathology and Immunohistochemical Staining

The spleen and brain tissues were fixed in 4% paraformaldehyde, and 5-μm paraffin sections prepared on PLL coat slides with microtome. To measure vacuolation in brain, the tissue sections were stained with hematoxylin and eosin (HE). In PrP^{Sc} staining, after deparaffinization and rehydration, the sections were pretreated by hydrated autoclaving at 121 °C for 15 min in 1 or 1.2 mM hydrochloric acid (17), followed by immersion in 90% formic acid for 5 min (25) to enhance PrP visualization, according to the protocol described by Brown et al (9). Endogenous peroxidase activity was inhibited with 0.3% hydrogen peroxidase in methanol for 30 min. Nonspecific binding sites of the primary antibody SAF32 (SPI-BIO, Montigny le Bretonneux, France) was blocked by preincubation in normal rabbit serum at 1:20 (Dako, Glostrup, Denmark) for 30 min, and then optimally titrated and diluted to 1:5000 and 1:500 (26, 32). The negative control sections were incubated with normal mouse IgG1 and IgG2b serum (DAKO) and then exposed to the primary antibodies overnight at room temperature. For determining follicular dendritic cell population in the spleen, we used anti-FDC antibody CNA.42 (DAKO) (31) and normal mouse IgM serum (DAKO) as a negative control for primary antibodies, and Histofine mouse stain kit (Nichirei biosciences, Inc., Jpn) for the secondary antibody. In glial staining, primary antibodies of anti-GFAP (glial fibrillary acidic protein) (DAKO) for the detection of activated astrocyte, and anti-Iba-1 (WAKO, Japan) for activated microglia were used. The secondary antibodies were Envision-mouse or rabbit HRP (DAKO) used at 1:200 for 1 h. Finally, the samples were stained with 0.025% 3,3' diaminobenzidine (DAB, Dojindo Lab, Japan) to visualize the reaction product, and counterstained with hematoxylin. The pattern of vacuolation, PrP^{Sc} deposits and gliosis were examined in 5 areas, namely the cortex, hippocampus, thalamus, cerebellum, and Pons. In semi-quantitative evaluation of spongiosis and gliosis, lesion severity of vacuolation as spongiform degeneration was scored on a 0–5 scale (non-detectable, a few, mild, moderate, severe and status spongiosus). PrP^{Sc} deposit was scored on a 0–4 scale (non-detectable, a few, mild, moderate and severe).

JVI Accepts published online ahead of print

Microgliosis and astrogliosis were scored on a 0–3 scale (non-detectable, mild, moderate and severe) and the values for each brain region were averaged.

Statistical analysis

The Student's t-test and Mann-Whitney U-test were used for comparison between two groups, and the one-way ANOVA followed by the Tukey-Kramer test, for multiple comparisons. The log rank test was used to analyze mortality of prion-infected mice. The correlation between parameters was determined by simple regression analysis and Peason's correlation coefficient test. Statistical analysis of all data was performed using the Statcel 2 on Excel and GraphPad Prism software.

Acknowledgments

We thank Dr. Tadatsugu Taniguchi for the gift of IRF3 knockout mice; and Drs. Hitoki Yamanaka, Takehiro Matsubara, Kazunori Sano, for helpful discussions and critical assessment of the manuscript; and Mari Kudo, Ayumi Yamakawa and Atsuko Matsuo, for technical assistance. This work was supported in part by the global COE Program (F12); a Grant-in-Aid for Young Scientists (B) (No. 22790955) from the Ministry of Education, Culture, Sports, Science, and Technology of Japan; a grant for BSE research, and a grant-in-aid of the Research Committee of Prion disease and Slow Virus Infection, from the Ministry of Health, Labor and Welfare of Japan.

JVI Accepts published online ahead of print

366 **FIGURE LEGENDS**

367 **Fig. 1.** Acceleration of prion pathogenesis in IRF3-/- mice.
368 (A) Survival curves in wild-type (+/+) (n=9, circle) and IRF3 knockout (-/-) (n=5,
369 triangle) mice after i.p. inoculation of 10^{-3} dilution of 22L-BH are plotted. The
370 difference between the two groups is statistically significant ($p < 0.05$, Logrank test).
371 (B) Accumulation of PrP^{Sc} in the brain tissues from wild-type or IRF3-/- mice was
372 analyzed by Western blotting. Molecular mass markers are indicated in kilodaltons
373 (kDa) on the left side of each panel. (C) PrP^{Sc} deposits were similarly stained in cortex
374 area of wild-type (+/+) and IRF3 knockout (-/-) mice at the terminal stages (upper
375 panels). There were no significant differences between wild-type and IRF3-/- mice in
376 the staining levels of PrP^{Sc} in the five brain regions: cortex (Cx), hippocampus (Hi),
377 thalamus (TH), cerebellum (CE) and Pons (Po) (lower graph). Scale-bars equal 25 μm.
378 All data are representative of at least three mice.
379
380 **Fig. 2.** Comparison of spongiform change between wild-type and IRF3-/- mice after
381 22L prion infection.
382 (A) Sections of the cortex (Cx) and cerebellum (CE) stained with hematoxylin and eosin
383 from wild-type (+/+) and IRF3 knockout (-/-) mice at 0, 25 w.p.i. and terminal stages
384 after i.p. inoculation of 10^{-3} dilution of 22L-BH are shown. Scale-bars equal 25 μm. (B)
385 Vacuolation scores in the same five brain regions as Fig. 1B were compared between
386 the prion-inoculated wild-type (circle) and IRF3-/- (triangle) mice at 25 w.p.i. or the
387 terminal stages. Statistical significance was determined using a two-tailed Student's
388 *t*-test. ***$p < 0.001$, *$p < 0.05$ compared with wild-type mice. Error bars indicate SEM.
389 These results are representative of at least three mice.
390
391 **Fig. 3.** Histopathological examination of gliosis in the brains of prion-infected mice.
392 (A) Immunohistochemical staining for Iba-I with hematoxylin counterstaining was
393 performed. The sections of cortex from wild-type (+/+) and IRF3 knockout (-/-) mice at
394 0, 25 w.p.i. and terminal stages are shown (upper panels). Lesion profiles of
395 microgliosis in the same five brain regions as Fig. 1B were compared between the
396 prion-inoculated wild-type (circle) and IRF3-/- (triangle) mice at the terminal stages
397 (lower graph). No significant differences were observed between the two groups at 25

JVI Accepts published online ahead of print

w.p.i. or at the terminal stage. (B) Immunostaining for GFAP with hematoxylin counterstaining (upper panels), and lesion profiles of astrogliosis (lower graph). Significant differences were observed between the two groups in Cx and CE regions at 25 w.p.i., but not at the terminal stage. Statistical significance was determined using a two-tailed Student's *t*-test. **p < 0.01, *p <0.05 compared with wild-type mice. Error bars indicate SEM. Scale-bars equal 25 μm. All results are representative of at least three mice.

Fig. 4. Early detection of PrP^{Sc} deposits in the spleen of prion-inoculated IRF3-/- mice. (A) Accumulation of PrP^{Sc} in the spleens was analyzed by immunohistochemistry (hydrophobic autoclaving method) at 5, 8 w.p.i. and terminal stages after i.p. inoculation of 10^{-3} dilution of 22L-BH. Scale-bars equal 25 μm. (B) The sections of spleen from wild-type (+/+) and IRF3 knockout (-/-) 5-week-old mice were stained with anti-FDC antibody (CNA.42). IgM is a negative control for the primary antibody. Scale-bars equal 20 μm.

Fig. 5. Inhibitory effect of IRF3 on PrP^{Sc} replication in cell culture. (A) Plasmids (pUNO) containing IRF3 gene were transiently transfected into 22L-N2a58 cells and incubated for 48 h. The panels on the left show PK-treated PrP as PrP^{Sc} (upper), total IRF3 (middle) and phosphorylated IRF3 (lower) in the cells. Mock, plasmids without IRF3 gene. The numbers above the panels represent the amount (μg) of the plasmids used for transfection. C, untransfected cells for negative control. The levels of PrP^{Sc} band intensity in the cells transfected with 4μg of the plasmids with or without IRF3 gene are expressed as a percentage compared with the control (right graph). The results in the graph are the mean ± SD of three independent experiments. Asterisks indicate statistically significant differences (*, $p < 0.05$). (B) The siRNAs of IRF3 were transfected into 22L-N2a58 cells and incubated for 48 h. The cells were subjected to Western blotting to detect PrP^{Sc}, β-actin and IRF3. The band intensities of PrP^{Sc} (middle graph) or IRF3/β-actin ratio (right graph) were quantified. Asterisks indicate statistically significant differences (*, $p < 0.05$ and **, $P < 0.01$). The data are representative of three independent experiments. (C) The effect of overexpression of HA-tagged IRF3 on new prion infection was analyzed using stable IRF3-overexpressing clones, A4, C1 and H3. A hygromycin-resistant but IRF3-negative clones, A1and E1,

JVI Accepts published online ahead of print

were used as the negative control. The top four panels show protein expression of PrP^C, total IRF3, HA-tagged IRF3 and β-actin prior to infection in each clone. After incubation with 0.02 % of 22L-BH for 48 h and then 5 passages, PrP^{Sc} levels in the clones were determined by Western blotting. The scatter diagram is indicative of a correlative relationship between the PrP^{Sc}/PrP^C ratio and the IRF3 expression ratio (right graph). A statistically significant ($P < 0.001$) correlation ($r = -0.8$) was observed between the PrP^{Sc} and the IRF3/β-actin ratio. The coefficient of determination is shown as R^2 values. All results are representative of at least three independent experiments, and each experiment was performed in triplicate.

REFERENCES

1. **Aguzzi, A., and M. Polymenidou.** 2004. Mammalian prion biology: one century of evolving concepts. Cell **116**:313-327.
2. **Akira, S., and K. Takeda.** 2004. Toll-like receptor signalling. Nat Rev Immunol **4**:499-511.
3. **Akira, S., S. Uematsu, and O. Takeuchi.** 2006. Pathogen recognition and innate immunity. Cell **124**:783-801.
4. **Arima, K., N. Nishida, S. Sakaguchi, K. Shigematsu, R. Atarashi, N. Yamaguchi, D. Yoshikawa, J. Yoon, K. Watanabe, N. Kobayashi, S. Mouillet-Richard, S. Lehmann, and S. Katamine.** 2005. Biological and biochemical characteristics of prion strains conserved in persistently infected cell cultures. J Virol **79**:7104-7112.
5. **Atarashi, R., V. L. Sim, N. Nishida, B. Caughey, and S. Katamine.** 2006. Prion strain-dependent differences in conversion of mutant prion proteins in cell culture. J Virol **80**:7854-7862.
6. **Au, W. C., P. A. Moore, W. Lowther, Y. T. Juang, and P. M. Pitha.** 1995. Identification of a member of the interferon regulatory factor family that binds to the interferon-stimulated response element and activates expression of interferon-induced genes. Proceedings of the National Academy of Sciences of the United States of America **92**:11657-11661.